

An approach for evaluation of EVD and small failure probabilities of uncertain nonlinear structures under stochastic seismic excitations

Chao Dang^a, Pengfei Wei^{a,b,*}, Michael Beer^{a,c,d}

^a*Institute for Risk and Reliability, Leibniz University Hannover, Callinstr. 34, Hannover 30167, Germany*

^b*School of Mechanics, Civil Engineering and Architecture, Northwestern Polytechnical University, Xi'an 710072, PR China*

^c*Institute for Risk and Uncertainty, University of Liverpool, Liverpool L69 7ZF, United Kingdom*

^d*International Joint Research Center for Engineering Reliability and Stochastic Mechanics, Tongji University, Shanghai 200092, PR China*

Abstract

Efficient assessment of small first-passage failure probabilities of nonlinear structures with uncertain parameters under stochastic seismic excitations is an important but still challenging problem. In principle, the first-passage failure probabilities can be evaluated once the extreme value distribution (EVD) of studied structural response becomes available. With this in mind, this study presents a novel approach, termed as *moment-generating function based mixture distribution* (MGF-MD), for evaluation of the EVD. In this method, the MGF is firstly introduced to characterize the EVD, and the advantages of this characterization are highlighted. To calculate the MGF defined by a high-dimensional expectation integral, a low-discrepancy sampling technique, named Latinized partially stratified sampling (LPSS), is employed with a small sample size. Besides, the unbiasedness of the estimator is proven and the confidence interval is given. Then, a mixture of two generalized inverse Gaussian distributions (MTGIGD) with a closed-form MGF is proposed to approximate the EVD from the knowledge of its estimated MGF. The parameter estimation is conducted by matching the MGF of MTGIGD with seven values of the estimated one. Three numerical examples, including the EVD of random variables and reliability evaluation of two uncertain nonlinear structures subjected to fully non-stationary stochastic ground motions, are studied. Results indicate that the proposed approach can provide reasonable accuracy and efficiency and is applicable to very high-dimensional systems with small failure probabilities.

Keywords: Extreme value distribution, Small first-passage probability, Moment-generating function, Mixture distribution, Generalized inverse Gaussian distribution, Nonlinear structure, Stochastic seismic excitation

*Corresponding author at: School of Mechanics, Civil Engineering and Architecture, Northwestern Polytechnical University, Xi'an 710072, PR China

Email addresses: chao.dang@irz.uni-hannover.de (Chao Dang), pengfeiwei@nwpu.edu.cn (Pengfei Wei), beer@irz.uni-hannover.de (Michael Beer)

Abbreviations

C.O.V.	coefficient of variation	MCS	Monte Carlo simulation
CDF	cumulative distribution function	MD	mixture distribution
DOF	degree of freedom	MEM	maximum entropy method
DPIM	direct probability integral method	MGF	moment-generating function
EVD	extreme value distribution	MTGIGD	mixture of two generalized inverse Gaussian distributions
FMNT	fourth-moment normal transformation	MTSND	mixture of two skew normal distributions
GEVD	generalized extreme value distribution	PDEM	probability density evolution method
GIGD	generalized inverse Gaussian distribution	PDF	probability density function
GPD	generalized Pareto distribution	POE	probability of exceedance
i.i.d.	independent and identically distributed	SGLD	shifted generalized lognormal distribution
IGD	inverse Gaussian distribution	SS	subset simulation
LPSS	Latinized partially stratified sampling	Std.D	standard deviation
LSS	Latinized stratified sampling		

1. Introduction

Efficient assessment of reliability of engineering structures in the presence of various uncertainties is an important task not only in the entire design process, but also in the whole service life. In order to ensure the seismic safety, the dynamic reliability analysis of structures under stochastic seismic excitations is usually formulated as the well-known first-passage failure problem [1, 2]. That is, the failure occurs once the studied stochastic structural response exceeds the prescribed threshold during a given time interval. Many efforts have been devoted to evaluating the first-passage probability of stochastic dynamic systems, such as the out-crossing rate based methods [3, 4], stochastic averaging [5, 6], path integration [7, 8], etc. The first-passage problem nevertheless still remain one of the most difficult issues

33 in stochastic dynamics due to the existence of several challenges. First of all, uncertainties arising from both the
34 earthquake loads and structural properties should be reasonably addressed simultaneously, which commonly results
35 in high dimensions of the reliability problem to be solved. The performance functions of structures may also exhibit
36 highly nonlinear behavior especially when subjected to strong earthquakes. Besides, as the structural systems become
37 increasingly complex, the existence of multiple underlying failure modes with dependencies further increases the
38 complexity of the problem. Apart from those challenges, the failure probabilities are typically expected to be very
39 small, e.g., the order of magnitude 10^{-4} or smaller.

40 The extreme value distribution (EVD) of stochastic structural response has attracted considerable attention since
41 the first-passage failure probabilities under different prescribed thresholds can be obtained equivalently through the as-
42 sociated EVD. Further, with the EVD, the time-dependent dynamic reliability problem can be conveniently converted
43 into a time-invariant counterpart. In this setting, some well-known reliability analysis methods could be directly in-
44 voked to address the above-mentioned challenges, e.g., the Monte Carlo simulation (MCS) and Subset Simulation
45 (SS) [9, 10] owing to their robustness to the dimension and complexity of the problem. However, the MCS is largely
46 restricted by its computational cost, especially for a expensive-to-evaluate model with a low level of failure proba-
47 bility. The SS offers noticeably improved efficiency compared to the MCS, but is still far away from desirable for
48 real-world applications. The present study particularly focuses on the evaluation of the entire EVD with efficiency and
49 accuracy. Usually, two kinds of approaches have been developed for deriving the EVD of a stochastic structural re-
50 sponse, i.e., the analytical approach and approximate approach. The analytical approaches are usually only applicable
51 for some specific types of stochastic processes [11, 12, 13, 14], thus are infeasible for general engineering problems
52 with the above-mentioned features/challenges. Alternatively, two major types of approximate approaches are avail-
53 able to capture the EVD: parametric approach and non-parametric approach. The basic idea of parametric approach
54 is to assume that the extreme value samples coming from a population can be adequately modeled by a probability
55 distribution with a fixed set of parameters. Based on the extreme value theory, the Gumbel distribution is used to
56 model the main body and tail behavior of the EVD [15, 16], followed by the generalized extreme value distribution
57 (GEVD) and generalized Pareto distribution (GPD) [17]. Among them, the GEVD could be more flexible, but still
58 restricted by its limitations. Besides, some four-parameter distributions are also developed to recover the EVD from

59 the knowledge of its first-four moments, e.g., the fourth-moment normal transformation (FMNT) [18] and shifted
60 generalized lognormal distribution (SGLD) [19]. Although these two models are generally versatile, the requirement
61 of estimating the response moments with high accuracy and efficiency is still a challenging task. With the emergence
62 of fractional moments, the maximum entropy method [20, 21, 22], kernel density maximum entropy method [23] and
63 mixture distribution [24] are proposed. Despite these, other non-standard parametric methods can also be found in the
64 literature [25, 26, 27]. For the non-parametric approach, assumptions on the distribution type of EVD are not requi.
65 The probability density evolution method (PDEM) can be employed to evaluate the EVD by constructing a virtual
66 stochastic process associated to the extreme value of the studied stochastic process [28, 29]. Recently, the direct
67 probability integral method (DPIM) [30] is proposed for stochastic response analysis of static and dynamic structural
68 systems based on the principle of probability conservation, which could also be used to capture the EVD of stochastic
69 response process. The PDEM and DPIM are generally applicable to strongly nonlinear systems, which, however, are
70 not easy to extend for problems with high-dimensional random inputs and small failure probabilities. In summary,
71 the success of the parametric approach relies on assumptions of the distributional type and methods for parameter
72 estimation. In other words, a good approximation can yield desirable results with less computational efforts. On the
73 contrary, the non-parametric approach is distribution-free, but still suffers from several drawbacks.

74 The main objective of the present study is to develop an efficient approach for assessment of the EVD and small
75 first-passage failure probabilities of nonlinear structures with uncertain parameters under stochastic seismic excita-
76 tions. For this purpose, the moment-generating function (MGF) is firstly introduced to characterize the EVD, instead
77 of the commonly-used integer moments and fractional moments. To calculate the MGF that is defined by a high-
78 dimensional expectation integral, the latinized partially stratified sampling (LPSS) is employed with a uced number
79 of samples due to its simultaneous variance uction associated with both main effects and variable interactions [31].
80 Then, a flexible mixture of two generalized inverse Gaussian distributions (MTGIGD) is proposed to recover the EVD
81 from the knowledge of its estimated MGF, where a MGF-matching technique is developed for parameter estimation.
82 Once the EVD is reconstructed in the entire distribution domain with reasonable accuracy, the first-passage failure
83 probabilities under different thresholds can be obtained without difficulty.

84 The rest of this paper is arranged as follows. Section 2 outlines the EVD-based method for first-passage failure

85 probabilities evaluation of stochastic dynamic systems. The MGF is introduced in Section 3 to characterize the EVD,
 86 the advantages and numerical approximation of which are also elaborated. In Section 4, a mixture distribution is
 87 developed to recover the EVD from its estimated MGF. Three numerical examples are investigated to validate the
 88 proposed approach in Section 5. Some concluding remarks are available in Section 6.

89 2. First-passage probability: an EVD perspective

90 Without loss of generality, consider a generic stochastic dynamic structural system governed by the following state
 91 equation and initial condition:

$$\dot{\mathbf{X}} = \mathbf{A}(\mathbf{X}, \boldsymbol{\Theta}, t), \mathbf{X}(t)|_{t=0} = \mathbf{x}_0 \quad (1)$$

92 where $\mathbf{X} = (X_1, X_2, \dots, X_d)^T$ is a d -dimensional state vector; $\mathbf{A} = (A_1, A_1, \dots, A_d)^T$ is the state mapping;
 93 $\boldsymbol{\Theta} = (\theta_1, \theta_2, \dots, \theta_n)^T$ denotes a n -dimensional random vector with known joint PDF $p_{\boldsymbol{\Theta}}(\boldsymbol{\theta})$, which might arise
 94 from both the system properties and external excitations. In general, the system properties might originally occur as
 95 stochastic fields or directly as some random parameters. Besides, it is widely recognized that the random seismic
 96 excitations should be modelled as non-stationary stochastic processes or fields [32]. The stochastic fields or pro-
 97 cesses can usually be further decomposed to a set of standard random variables, e.g., by K-L expansion [33] and
 98 spectral representation method [34]. Therefore, a large number of random variables could be involved in a dynamic
 99 structural system with uncertain parameters subjected to non-stationary stochastic seismic excitations, leading to a
 100 high-dimensional system to be handled.

101 For a well-posed dynamical system, it is reasonable to assume that the solution to Eq. (1) exists uniquely as a
 102 function of $\boldsymbol{\Theta}$, which is expressed as:

$$\mathbf{X}(t) = \mathbf{H}(\boldsymbol{\Theta}, t), \dot{\mathbf{X}}(t) = \mathbf{h}(\boldsymbol{\Theta}, t) \quad (2)$$

103 where \mathbf{H} and $\mathbf{h} = \partial\mathbf{H}/\partial t$ are the deterministic operators.

104 If there are a set of system response quantities of interest $\mathbf{Q}(t) = (Q_1(t), Q_2(t), \dots, Q_m(t))^T$ for reliability
 105 analysis, such as the inter-story drifts and strains or stresses at some points, then \mathbf{Q} can usually be calculated from its

106 connection with the state vectors. It is convenient to assume that the relationship takes the form:

$$\mathbf{Q}(t) = \Psi \left[\mathbf{X}(t), \dot{\mathbf{X}}(t) \right] = \mathbf{W}(\boldsymbol{\Theta}, t) \quad (3)$$

107 where Ψ is a transfer operator; \mathbf{W} denotes a mapping from $\boldsymbol{\Theta}$ to \mathbf{Q} . Alternatively, Eq. (3) can be expressed as its
108 component form:

$$Q_l(t) = W_l(\boldsymbol{\Theta}, t), \quad l = 1, 2, \dots, m \quad (4)$$

109 For notational simplicity, the subscript l will be omitted hereafter without inducing confusions.

110 In general, the first-passage reliability is defined as:

$$P_r = \Pr\{Q(t) \in \Omega_s, t \in [0, T]\} \quad (5)$$

111 where $\Pr\{\cdot\}$ is the probability operator; Ω_s is the safe domain; T is the duration of time. For the case of symmetric
112 double-boundary safe domain concerned in this study, the first-passage reliability can be further written as:

$$P_r = \Pr\{|Q(t)| < b, t \in [0, T]\} \quad (6)$$

113 where b is the prescribed threshold. Since $Q(t)$ can be a general stochastic response process, evaluation of P_r remains
114 a non-trivial task, especially for a expensive-to-evaluate model.

115 Let Z denote the maximum value of $|Q(t)|$, i.e.

$$Z = \max_{t \in [0, T]} |Q(t)| = \max_{t \in [0, T]} |W(\boldsymbol{\Theta}, t)| = G(\boldsymbol{\Theta}) \quad (7)$$

116 Note that Z is conveniently assumed to be as a function of $\boldsymbol{\Theta}$ and should be a positive random variable in this form.

117 Then, Eq. (6) is equivalent to:

$$P_r = \Pr\{Z = G(\boldsymbol{\Theta}) < b\} \quad (8)$$

118 That is to say, once the probability distribution of Z is available, which is refer to as the extreme value distribution
119 (EVD), P_r can be straightforwardly and conveniently obtained. Denote the probability density function (PDF) and
120 cumulative distribution function (CDF) of Z as $f_Z(z)$ and $F_Z(z)$, respectively, and then the first-passage reliability
121 is:

$$P_r = \int_{-\infty}^b f_Z(z) dz = F_Z(b) \quad (9)$$

122 and the corresponding failure probability is

$$P_f = \int_b^{+\infty} f_Z(z) dz = 1 - F_Z(b) \quad (10)$$

123 The problem of first-passage reliability is now equivalently transformed to evaluation of the EVD. Despite of the
 124 conceptual elegance, it is still not easy to directly derive the analytical PDF or CDF of the EVD of a general stochastic
 125 response process. To address this challenge, an efficient approach will be developed in the following sections to
 126 capture the EVD.

127 3. Moment-generating function of the EVD

128 To characterize the EVD, the statistical moments, such as the mean value and variance, are commonly employed
 129 in the literature. However, it is known that the probabilistic information from the low-order moments is not sufficient
 130 to accurately capture an unknown distribution. Additionally, the high-order moments, e.g., the skewness and kursto-
 131 sis, containing more information regarding the tail behavior are consider for a more accurate characterization [18].
 132 Nevertheless, high-order moments are invariably complicated to analyze and sampling variability of power moments
 133 increases with the order of moment. Recently, the fractional moments with low-order exponents are introduced pri-
 134 marily due to the fact that even a single low-order fractional moment can contain a large amount of information on
 135 numerous integer moments [24]. Even so, it is worth mentioning that either a finite sequence of integer moments or
 136 fractional moments can not uniquely determine a underlying probability distribution. Based on those considerations,
 137 the moment-generating function will be introduced in this work to characterize the EVD.

138 3.1. Definition of the moment-generating function

139 For the positive random variable Z defined in Eq. (7), its moment-generating function (MGF) can by expressed
 140 as:

$$M_Z(\tau) = \mathbb{E} [e^{\tau Z}] = \int_0^{+\infty} e^{\tau z} f_Z(z) dz, \tau \in \mathbb{R} \quad (11)$$

141 where $\mathbb{E}[\cdot]$ denotes the expectation operator.

142 Consider the series expansion of $e^{\tau Z}$

$$e^{\tau Z} = 1 + \tau Z + \frac{\tau^2 Z^2}{2!} + \frac{\tau^3 Z^3}{3!} + \cdots + \frac{\tau^r Z^r}{r!} + \cdots \quad (12)$$

143 and hence

$$M_Z(\tau) = 1 + \tau \mathbb{E}[Z] + \frac{\tau^2 \mathbb{E}[Z^2]}{2!} + \frac{\tau^3 \mathbb{E}[Z^3]}{3!} + \dots + \frac{\tau^r \mathbb{E}[Z^r]}{r!} + \dots \quad (13)$$

144 where $\mathbb{E}[Z^r]$ is the r -th moment of Z . Eq. (13) implies that the MGF at any non-zero τ includes a bulk of probabilistic
145 information on infinite number of integer moments. This feature is similar to that of fractional moments, while
146 fractional moments only make sense with positive random variables.

147 Further, the r -th moment of Z can be obtained from its MGF such that:

$$\mathbb{E}[Z^r] = M_Z^{(r)}(0) = \left. \frac{d^r M_Z}{d\tau^r} \right|_{\tau=0} \quad (14)$$

148 Eq. (14) implies that only the MGF near the origin already contains all the information for any order of integer
149 moment. The MGF is so named because all moments of Z can be computed from its derivative evaluated at $\tau = 0$.
150 However, it is impossible to obtain any order integer moment from a single fractional moment (not the integer moment
151 itself), even though it includes the information conceptually.

152 Besides, the MGF (if it exists) can uniquely determine the underlying distribution (see Section 30 of [35]). In
153 other words, if two random variables have the same MGF, then they must follow the same distribution. Thus, the
154 MGF characterization of the EVD is more suitable than traditional integer moments or fractional moments. For more
155 properties concerning the MGF, please refer to, e.g., [36].

156 3.2. Numerical approximation of the moment-generating function

157 For the EVD of a general stochastic response process, derivation of closed-form solution of its MGF is not trivial.
158 Therefore, numerical evaluation is necessary for general applications. For our purpose, the MGF defined in Eq. (11)
159 can be further expressed as:

$$M_Z(\tau) = \int_{\mathcal{D}_{\boldsymbol{\theta}}} e^{\tau G(\boldsymbol{\theta})} p_{\boldsymbol{\theta}}(\boldsymbol{\theta}) d\boldsymbol{\theta} \quad (15)$$

160 where $\mathcal{D}_{\boldsymbol{\theta}}$ is the distribution domain of $\boldsymbol{\theta}$. As the dimension of $\boldsymbol{\theta}$ could be very large, $M_Z(\tau)$ is generally a
161 high-dimensional integral with a complicated integrand.

162 To evaluate such an integral, a recently developed low-discrepancy sampling technique, named Latinized partially

163 stratified sampling (LPSS) [31], will be employed. Eq. (15) can be estimated by the following estimator:

$$\hat{M}_Z(\tau) = \frac{1}{N} \sum_{i=1}^N e^{\tau G(\boldsymbol{\theta}^{(i)})} \quad (16)$$

164 where N is the total number of samples; $\{\boldsymbol{\theta}^{(i)}\}_{i=1}^N$ are a set of samples of $\boldsymbol{\theta}$. Since LPSS method is originally
 165 designed for generating uniformly distributed samples over the unit hypercube, i.e, $\mathcal{D}_U = [0, 1]^d$, a transformation
 166 $\boldsymbol{\theta}^{(i)} = T(\mathbf{u}^{(i)})$ should be applied to obtain the sample $\boldsymbol{\theta}^{(i)}$ from $\mathbf{u}^{(i)}$ ($\{\mathbf{u}^{(i)}\}_{i=1}^N$ are a set of samples generated
 167 by LPSS). A novel feature of the LPSS is that it can reduce the variance related to the main effects and variable
 168 interactions simultaneously, and hence a reduced set of samples could be sufficient to accurately evaluate the MGF.
 169 Readers may refer to [31] for technical details and [24, 37] for implementation issues of the LPSS method. The basic
 170 algorithm is presented in Algorithm 1. The Matlab code is readily available at: [https://www.mathworks.co](https://www.mathworks.com/matlabcentral/fileexchange/54847-latinized-partially-stratified-sampling)
 171 [m/matlabcentral/fileexchange/54847-latinized-partially-stratified-sampling](https://www.mathworks.com/matlabcentral/fileexchange/54847-latinized-partially-stratified-sampling).

Algorithm 1 Latinized partially stratified sampling

- 1: **Input:** Specify the sample size N , number of dimensions d and orthogonal subspaces $\mathcal{S}_j (j = 1, 2, \dots, L)$, where
 $\mathcal{S}_{j_1} \perp \mathcal{S}_{j_2} (j_1 \neq j_2)$ and $\mathcal{S}_1 \oplus \mathcal{S}_2 \oplus \dots \oplus \mathcal{S}_L = \mathcal{D}_U$.
 - 2: For each subspace \mathcal{S}_j , generate N low-dimensional samples using Latinized stratified sampling (LSS) [31].
 - 3: Randomly select a sample from each subspace (without replacement) and group the selected samples to produce
 a sample in d -dimensional space.
 - 4: Repeat step 3 until N samples are constructed in d -dimensional space.
 - 5: **Output:** N samples in d -dimensional unit hypercube.
-

172 Regardless of the distribution of Z , we have

$$\mathbb{E} \left[\hat{M}_Z(\tau) \right] = \mathbb{E} \left[\frac{1}{N} \sum_{i=1}^N e^{\tau G(\boldsymbol{\theta}^{(i)})} \right] = \frac{1}{N} \sum_{i=1}^N \mathbb{E} \left[e^{\tau G(\boldsymbol{\theta}^{(i)})} \right] = \frac{1}{N} \sum_{i=1}^N M_Z(\tau) = M_Z(\tau) \quad (17)$$

173 Thus, the MGF estimator in Eq. (16) is proven to be unbiased. Further, the estimator will approximately follow the
 174 normal distribution with mean $\hat{\mu}(\tau) = \hat{M}_Z(\tau)$ and variance given by:

$$\hat{\sigma}^2(\tau) = \frac{1}{N(N-1)} \sum_{i=1}^N \left[e^{\tau G(\boldsymbol{\theta}^{(i)})} - \hat{M}_Z(\tau) \right]^2 \quad (18)$$

175 Confidence interval can then be obtained accordingly. For example, the 95% confidence interval of the estimator is as
 176 follows:

$$[\hat{\mu}(\tau) - 1.96\hat{\sigma}(\tau), \hat{\mu}(\tau) + 1.96\hat{\sigma}(\tau)] \quad (19)$$

177 Eq. (16) can be used to obtain a point estimate of the MGF. In order to inform the accuracy of the point estimate,
 178 Eq. (19) gives a interval estimate of the MGF, which actually reflects the sampling variability and can be narrowed by
 179 increasing the sample size N .

180 4. Recovering the EVD from its moment-generating function by a mixture distribution

181 In this section, the problem of how to find the underlying EVD from the knowledge of its estimated MGF is
 182 studied. Although the MGF can uniquely determine a probability distribution, it is not easy to deduce the underlying
 183 distribution directly. Alternatively, we focus on offering an efficient and accurate parametric approach to approximate
 184 the EVD. For this purpose, a flexible mixture distribution will be developed on the basis of the generalized inverse
 185 Gaussian distribution, and then the parameter estimation based on the MGF is elaborated.

186 4.1. Generalized inverse Gaussian distribution

187 The generalized inverse Gaussian distribution (GIGD) is a three-parameter family of continuous probability dis-
 188 tributions, which has a wide variety of applications in many fields. A random variable has a GIGD if its PDF is given
 189 by [38]:

$$f_{\text{GIGD}}(z; \alpha, \beta, \lambda) = \frac{(\alpha/\beta)^{\lambda/2}}{2K_{\lambda}(\sqrt{\alpha\beta})} z^{(\lambda-1)} e^{-(\alpha z + \beta/z)/2}, z > 0 \quad (20)$$

190 where $\alpha > 0$, $\beta > 0$ and $\lambda \in \mathbb{R}$ are the three parameters; K_{λ} is a modified Bessel function of the second kind with
 191 order λ .

192 The inverse Gaussian distribution (IGD) is a special case of GIGD when $\lambda = -1/2$. The special and limiting cases
 193 of the IGD also belong to the GIGD, such as the normal distribution and Lévy distribution. Besides, other special
 194 cases include the hyperbolic distribution for $\lambda = 0$, Gamma distribution for $\beta \rightarrow 0$ and inverse-gamma distribution
 195 for $\alpha \rightarrow 0$.

196 The closed-form solution of the MGF of GIGD exists and reads:

$$M_{\text{GIGD}}(\tau; \alpha, \beta, \lambda) = \left(\frac{\alpha}{\alpha - 2\tau} \right)^{\frac{\lambda}{2}} \frac{K_{\lambda}(\sqrt{\beta(\alpha - 2\tau)})}{K_{\lambda}(\sqrt{\alpha\beta})} \quad (21)$$

197 Based on the MGF, the mean and variance can be obtained as:

$$\mu_{\text{GIGD}} = \frac{\sqrt{\beta} K_{\lambda+1}(\sqrt{\alpha\beta})}{\sqrt{\alpha} K_{\lambda}(\sqrt{\alpha\beta})} \quad (22)$$

$$\sigma_{\text{GIGD}}^2 = \left(\frac{\beta}{\alpha} \right) \left[\frac{K_{\lambda+2}(\sqrt{\alpha\beta})}{K_{\lambda}(\sqrt{\alpha\beta})} - \left(\frac{K_{\lambda+1}(\sqrt{\alpha\beta})}{K_{\lambda}(\sqrt{\alpha\beta})} \right)^2 \right] \quad (23)$$

198
199 The reason why we specially select the GIGD as the basis of the proposed parametric distribution model is mostly
200 based on the two following considerations. First of all, the GIGD is flexible in shapes and tail properties since several
201 theoretical distributions with distinct features are included (as mentioned early). It is worthy mentioning that the IGD
202 as a special case of the GIGD is the exact first-passage time distribution of the Brownian motion (Wiener process)
203 [39]. Second, the MGF of the GIGD is readily available in a closed form (Eq. (21)), which enables the deviation of
204 the MGF and parameter estimation of the proposed mixture distribution model (see the following two subsections).

205 4.2. A mixture of two generalized inverse Gaussian distributions

206 Although the GIGD is more versatile than the IGD by adding an extra free parameter, its flexibility should be
207 further enhanced to capture the EVD since more emphasis is placed on the tail, in addition to the main body of the
208 distribution, especially for evaluation of small first-passage failure probabilities. Finite mixture models allow us to
209 create new distributions with increased number of free parameters and hence flexibility in a simple, but efficient way
210 [40]. However, identification of free parameters is an intractable task as the number of mixture components increases,
211 since they usually cannot be derived explicitly. To this end, a mixture of two generalized inverse Gaussian distributions
212 (MTGIGD) will be specially developed to capture the EVD in the present work. The PDF of the MTGIGD is given
213 by:

$$\begin{aligned} f_{\text{MTGIGD}}(z; \Sigma) &= \varpi f_{\text{GIGD}}(z; \alpha^{(1)}, \beta^{(1)}, \lambda^{(1)}) + (1 - \varpi) f_{\text{GIGD}}(z; \alpha^{(2)}, \beta^{(2)}, \lambda^{(2)}) \\ &= \varpi \frac{(\alpha^{(1)}/\beta^{(1)})^{\lambda^{(1)}/2}}{2K_{\lambda^{(1)}}(\sqrt{\alpha^{(1)}\beta^{(1)}})} z^{(\lambda^{(1)}-1)} e^{-(\alpha^{(1)}x+\beta^{(1)}/z)/2} \\ &\quad + (1 - \varpi) \frac{(\alpha^{(2)}/\beta^{(2)})^{\lambda^{(2)}/2}}{2K_{\lambda^{(2)}}(\sqrt{\alpha^{(2)}\beta^{(2)}})} z^{(\lambda^{(2)}-1)} e^{-(\alpha^{(2)}x+\beta^{(2)}/z)/2} \end{aligned} \quad (24)$$

214 where $0 < \varpi < 1$ and $1 - \varpi$ are the mixture weights of the first and second mixture components, respectively; $\Sigma =$
 215 $[\varpi, \alpha^{(1)}, \beta^{(1)}, \lambda^{(1)}, \alpha^{(2)}, \beta^{(2)}, \lambda^{(2)}]^T$ is a set of seven free parameters to be determined; The superscript distinguishes
 216 those parameters from different mixture components.

217 The MGF of the MTGIGD can be derived as:

$$\begin{aligned}
 M_{\text{MTGIGD}}(\tau; \Sigma) &= \int_0^{+\infty} e^{\tau z} f_{\text{MTGIGD}}(z; \Sigma) dz \\
 &= \int_0^{+\infty} e^{\tau z} \left(\varpi f_{\text{GIGD}}(z; \alpha^{(1)}, \beta^{(1)}, \lambda^{(1)}) + (1 - \varpi) f_{\text{GIGD}}(z; \alpha^{(2)}, \beta^{(2)}, \lambda^{(2)}) \right) dz \\
 &= \varpi \int_0^{+\infty} e^{\tau z} f_{\text{GIGD}}(z; \alpha^{(1)}, \beta^{(1)}, \lambda^{(1)}) dz + (1 - \varpi) \int_0^{+\infty} e^{\tau z} f_{\text{GIGD}}(z; \alpha^{(2)}, \beta^{(2)}, \lambda^{(2)}) dz \\
 &= \varpi M_{\text{GIGD}}(\tau; \alpha^{(1)}, \beta^{(1)}, \lambda^{(1)}) + (1 - \varpi) M_{\text{GIGD}}(\tau; \alpha^{(2)}, \beta^{(2)}, \lambda^{(2)}) \\
 &= \varpi \left(\frac{\alpha^{(1)}}{\alpha^{(1)} - 2\tau} \right)^{\frac{\lambda^{(1)}}{2}} \frac{K_{\lambda^{(1)}}(\sqrt{\beta^{(1)}(\alpha^{(1)} - 2\tau)})}{K_{\lambda^{(1)}}(\sqrt{\alpha^{(1)}\beta^{(1)}})} \\
 &\quad + (1 - \varpi) \left(\frac{\alpha^{(2)}}{\alpha^{(2)} - 2\tau} \right)^{\frac{\lambda^{(2)}}{2}} \frac{K_{\lambda^{(2)}}(\sqrt{\beta^{(2)}(\alpha^{(2)} - 2\tau)})}{K_{\lambda^{(2)}}(\sqrt{\alpha^{(2)}\beta^{(2)}})}
 \end{aligned} \tag{25}$$

218 If we assume that the EVD follows the MTGIGD, i.e., $\hat{f}_Z(z) = f_{\text{MTGIGD}}(z; \Sigma)$, then how to estimate the unknown
 219 parameters collecting in Σ could be another critical task.

220 4.3. Moment-generating function based parameter estimation

221 The MGF of the EVD is obtained in Section 3 and the closed-form expression of MGF of the MTGIGD exists.
 222 A natural idea for estimating parameters is to match the EVD's MGF with that of the MTGIGD, and the following
 223 equations can be established accordingly:

$$\begin{cases}
 M_{\text{MTGIGD}}(\tau_1; \Sigma) = \hat{M}_Z(\tau_1) \\
 M_{\text{MTGIGD}}(\tau_2; \Sigma) = \hat{M}_Z(\tau_2) \\
 \dots \\
 M_{\text{MTGIGD}}(\tau_7; \Sigma) = \hat{M}_Z(\tau_7)
 \end{cases} \tag{26}$$

224 where $\{\tau_j\}_{j=1}^7$ are seven discrete values of τ . In fact, τ around zero is more concerned due to its high estimation
 225 accuracy and sufficient probabilistic information included. However, $\hat{M}_Z(\tau)$ could be sufficient large for $\tau > 0$, since
 226 Z is a positive random variable in the context of this article. For this reason, the discrete values of τ are adopted as

227 $\{\tau_j\}_{j=1}^7 = \{-0.1, -0.2, -0.3, -0.4, -0.5, -0.6, -0.7\}$ in this study. One can use the built-in function “fsolve” in
 228 Matlab to solve the above system of equations.

229 As a suggestion, the following estimates can be served as the initial values of the parameters as a guess:

$$\varpi = 0.4 \quad (27)$$

230

$$\alpha^{(1)} = \alpha^{(2)} = \frac{\hat{\mu}_Z}{\hat{\sigma}_Z^2} \quad (28)$$

231

$$\beta^{(1)} = \beta^{(2)} = \frac{\hat{\mu}_Z^3}{\hat{\sigma}_Z^2} \quad (29)$$

232

$$\lambda^{(1)} = \lambda^{(2)} = -\frac{1}{2} \quad (30)$$

233 where the parameters except for ω are estimated by the method of moments in the case that each mixture component
 234 is reduced to the IGD; $\hat{\mu}_Z$ and $\hat{\sigma}_Z^2$ are the estimated mean and variance of the EVD, which can be evaluated by:

$$\hat{\mu}_Z = \frac{1}{N} \sum_{i=1}^N G(\boldsymbol{\theta}^{(i)}) \quad (31)$$

235

$$\hat{\sigma}_Z^2 = \frac{1}{N-1} \sum_{i=1}^N \left(G(\boldsymbol{\theta}^{(i)}) - \hat{\mu}_Z \right)^2 \quad (32)$$

236 Note that no extra dynamic structural analysis is actually requi in this step.

237 Once the free parameters in the MTGIGD model are identified properly, one can obtain a point estimate of the
 238 EVD, and hence the first-passage failure probabilities under different prescribed thresholds. However, how to measure
 239 the accuracy of the results is a non-trivial task since both the sampling error containing in the MGF estimate and the
 240 model assumption error for functional form of the EVD should be addressed simultaneously. This is not attempted in
 241 this study, but we hope that our work will stimulate further studies.

242

243 The flowchart of the proposed approach for efficient assessment of EVD and first-passage failure probabilities of
 244 structures with uncertain parameters under stochastic seismic excitations is depicted in Fig. 1.

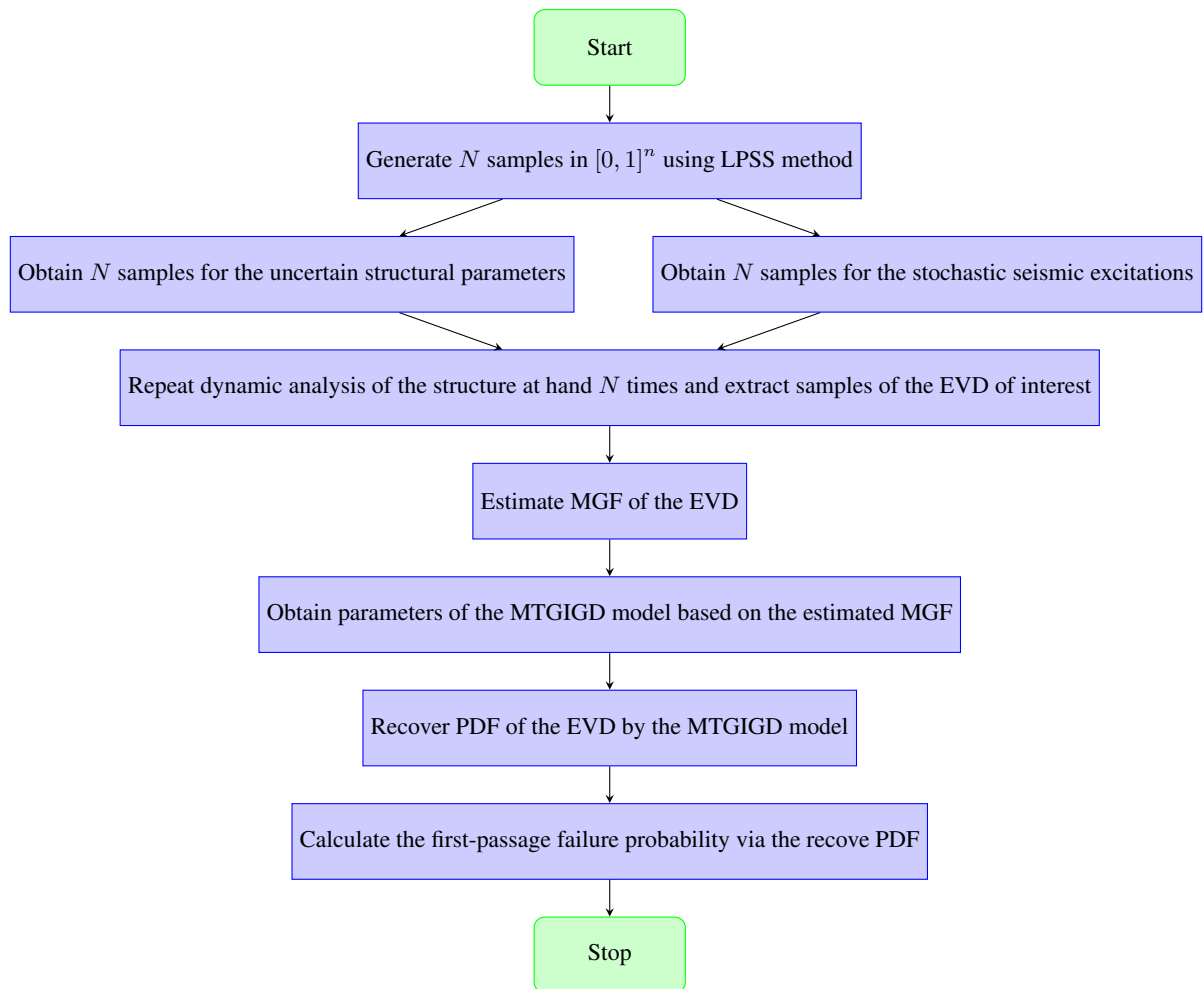


Figure 1: Flowchart of the proposed approach.

245 5. Numerical examples

246 To validate the proposed approach, three numerical examples will be presented in this section. In the first example,
247 the EVD of random variables is investigated where the analytical solution of the EVD is available. The EVD approx-
248 imated by the proposed method is verified through comparison with the analytical solution, indicating the accuracy
249 of the proposed method. The EVD of the response of two nonlinear structures with uncertain parameters subjected to
250 fully non-stationary stochastic seismic excitations is computed through the proposed approach, and the first-passage
251 failure probabilities under different prescribed thresholds are obtained in example 2 and 3. In comparison with Monte
252 Carlo simulation and other state-of-the-art methods, advantages of the proposed method are demonstrated.

253 5.1. Example 1: EVD of random variables

254 Suppose that $\mathbf{X} = [X_1, X_2, \dots, X_n]$ are i.i.d. standard normal random variables. Consider the maximum absolute
255 value such that:

$$Z = \max(|X_1|, |X_2|, \dots, |X_n|) \quad (33)$$

256 where $Y_i = |X_i|$ actually follows a folded standard normal distribution. Denote the PDF and CDF of Y_i as $f_Y(y)$
257 and $F_Y(y)$, respectively. According to the probability theory, the closed-form solutions of the PDF and CDF of Z are
258 available, and given by:

$$f_Z(z) = n f_Y(z) F_Y^{n-1}(z), F_Z(z) = F_Y^n(z) \quad (z \geq 0) \quad (34)$$

259 The proposed approach can also be employed to approximate the PDF and CDF of Z . Three cases, i.e., $n =$
260 1000, 3000, 5000, will be studied to verify the proposed method. First, the MGFs of Z are estimated by the LPSS
261 method with a small sample size of $N = 625$. The estimated MGFs are compared with those obtained by MCS
262 (with 10^6 runs), as shown in Fig. 2. It is observed that the confidence intervals are all very narrow, and contain the
263 results given by MCS, indicating the accuracy of LPSS method. The MTGIGD is then used to recover the PDF and
264 CDF of Z by fitting seven values of the estimated MGF. The recover PDF and CDF of those three cases are compa-
265 risoned with the analytical solutions in Figs. 3 - 5, respectively. Note that the two mixture components of the proposed
266 MIGIND multiplied by their corresponding mixture weights are also given. As seen, the recovered PDF and CDF

267 agree well with those analytical solutions. This example demonstrates the accuracy of the proposed method, as well
 268 as the efficiency for such three high-dimensional cases.

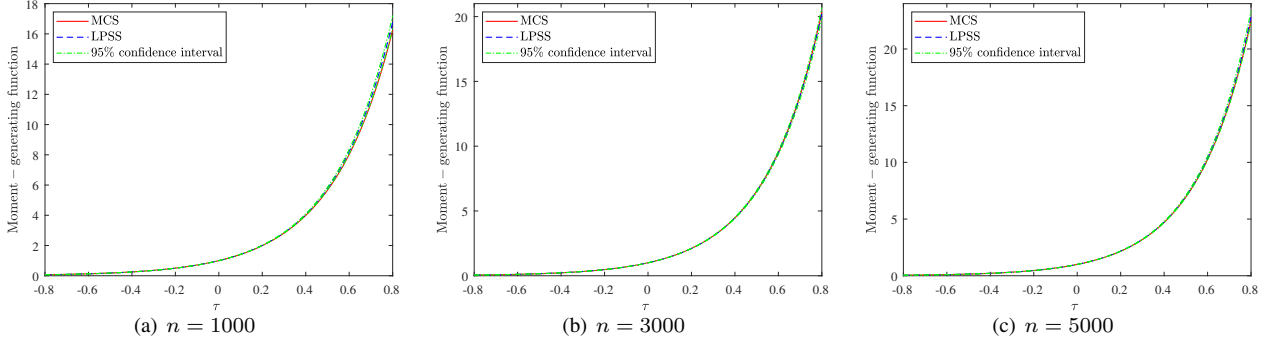


Figure 2: Moment-generating function of the EVD in Example 1.

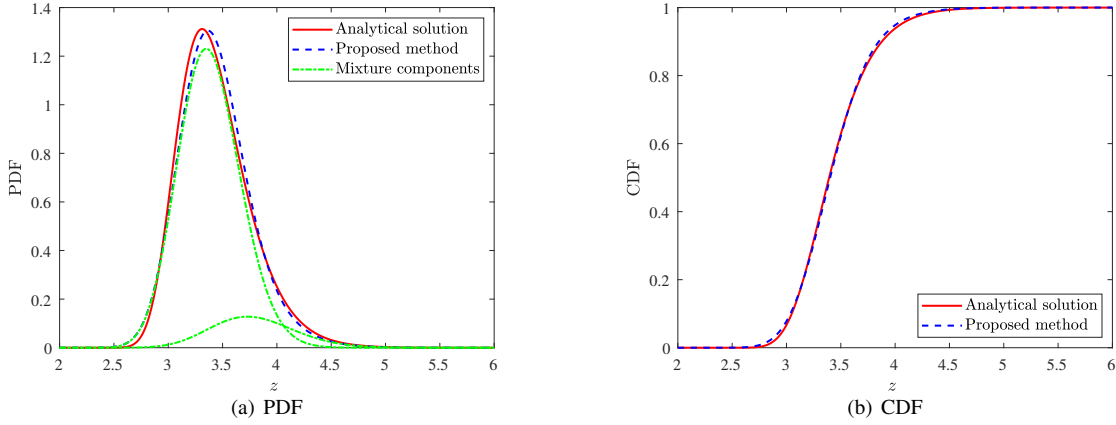


Figure 3: Comparison of PDF and CDF of the EVD in Example 1 ($n = 1000$).

269 **5.2. Example 2: EVD and first-passage failure probabilities of a nonlinear shear frame structure**

270 Consider a two-span ten-story nonlinear shear frame structure with uncertain parameters under stochastic seismic
 271 excitations, as shown in Fig. 6. The equation of motion of this structure is given by:

$$M(\boldsymbol{\theta})\ddot{\mathbf{X}}(t) + C(\boldsymbol{\theta})\dot{\mathbf{X}}(t) + K(\boldsymbol{\theta})[\varepsilon\mathbf{X}(t) + (1 - \varepsilon)\mathbf{Y}(t)] = -M(\boldsymbol{\theta})I\ddot{U}_g(\boldsymbol{\theta}, t) \quad (35)$$

272 where M , C and K are the mass, damping and initial stiffness matrices. Rayleigh damping is adopted such that
 273 $C = a_1M + a_2K$, where a_1 and a_2 are obtained by assuming the damping ratio $\xi = 5\%$ for the first two modes. The

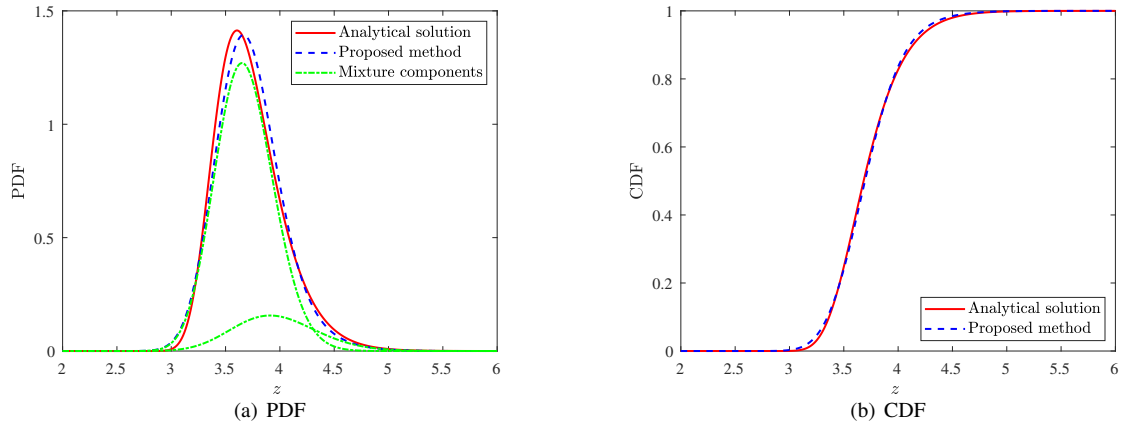


Figure 4: Comparison of PDF and CDF of the EVD in Example 1 ($n = 3000$).

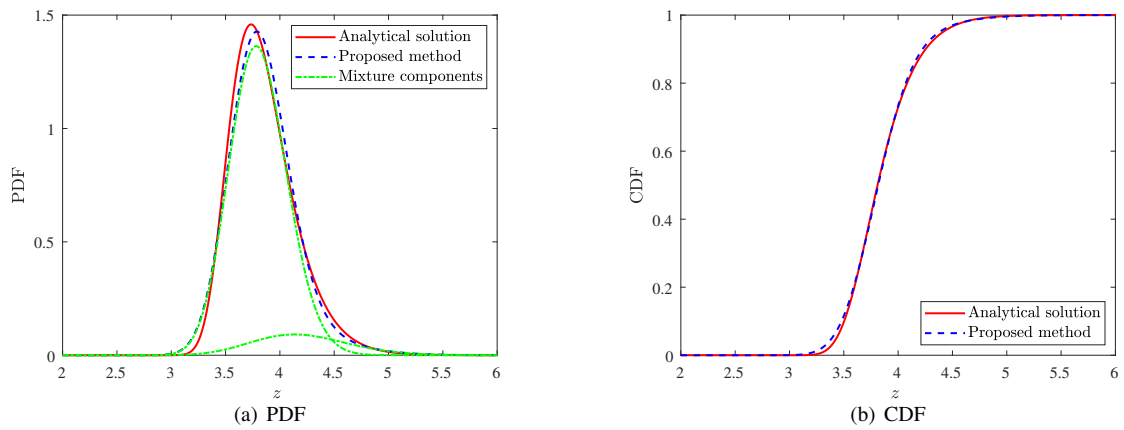


Figure 5: Comparison of PDF and CDF of the EVD in Example 1 ($n = 5000$).

274 lumped mass and inter-story stiffness of each story are assumed to be independent random variables, the probabilistic
 275 information of which is summarized in Tabs. 1 and 2, respectively. That is, $d_1 = 20$ random variables are involved in
 276 the uncertain structural properties. $\ddot{\mathbf{X}}(t)$, $\dot{\mathbf{X}}(t)$ and $\mathbf{X}(t)$ are the acceleration, velocity and displacement vectors. The
 277 parameter ε , that controls the degree of hysteresis, is set to be 0.20. The term $\mathbf{Y}(t)$ is characterized by the Bouc–Wen
 278 model [41, 42]:

$$\dot{\mathbf{Y}}(t) = \rho \dot{\mathbf{X}}(t) - \eta |\dot{\mathbf{X}}(t)| |\mathbf{Y}(t)|^{n_0-1} \mathbf{Y}(t) - \gamma \dot{\mathbf{X}}(t) |\mathbf{Y}(t)|^{n_0} \quad (36)$$

279 where ρ , η , γ and n_0 are dimensionless quantities, which control the behaviour of the model. These parameters take
 280 the following values: $\rho = 1$, $n_0 = 3$ and $\eta = \gamma = 1/(2u_y^{n_0})$, in which $u_y = 0.01$ m is the yielding displacement. I
 281 is the loading inference vector. The seismic excitation $\ddot{U}_g(t)$ is modeled by a fully non-stationary stochastic process
 282 via the spectral representation method [43]:

$$\ddot{U}_g(t) = \sum_{i=1}^{d_2} \sqrt{2S_{\ddot{u}_g}(\omega_i, t)\Delta\omega} (A_i \cos(\omega_i t) + B_i \sin(\omega_i t)) \quad (37)$$

283 where $S_{\ddot{u}_g}(\omega, t)$ is the evolutionary power spectral density (EPSD) function, which is defined as:

$$S_{\ddot{u}_g}(\omega, t) = |f(\omega, t)|^2 G(\omega) \quad (38)$$

284 in which $f(\omega, t)$ is the modulation function of time and frequency, given by:

$$f(\omega, t) = \exp\left(-\delta_0 \frac{\omega t}{\omega_a t_a}\right) \cdot \left[\frac{t}{c} \exp\left(1 - \frac{t}{c}\right)\right]^k \quad (39)$$

285 and $G(\omega)$ is the one-sided PSD, assumed to follow the Clough- Penzien spectrum:

$$G(\omega) = \frac{\omega_g^4 + 4\zeta_g^2 \omega_g^2 \omega^2}{(\omega_g^2 - \omega^2)^2 + (2\zeta_g \omega_g \omega)^2} \frac{\omega^4}{(\omega_f^2 - \omega^2)^2 + (2\zeta_f \omega_f \omega)^2} S_0 \quad (40)$$

286 $\{A_i, B_i\}_{i=1}^{d_2}$ in Eq. (37) are $2d_2$ independent standard normal random variables. In this example, $d_2 = 800$ is adopted,
 287 i.e., a total of $d = d_1 + 2d_2 = 1620$ random variables are included in Θ . Other involved parameters are specified
 288 as: $\Delta t = 0.02$ s, $T = 30$ s; $\Delta\omega = 0.15$ rad/s, $\omega_1 = 0.15$ rad/s, $\omega_u = 240$ rad/s; $\delta_0 = 0.15$, $c = 9.0$, $k = 2.0$;
 289 $\omega_g = 5\pi$ rad/s, $\zeta_g = \zeta_f = 0.60$, $\omega_f = 0.1\omega_g$, $S_0 = 54.6296$ cm²/s³.

290 The LPSS method is firstly employed to generate $N = 625$ sample points in $[0, 1]^d$ ($d = 1620$), serving as a basic
 291 point set. Then, these samples are transformed to the random-variate space of the vector Θ . Integrating the samples

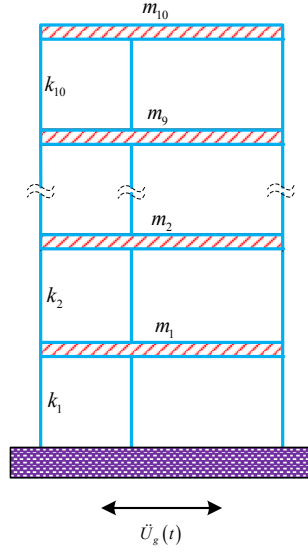


Figure 6: A two-bay ten-story shear frame structure subjected to stochastic seismic excitations.

Table 1: Probabilistic information of the lumped mass

Lumped mass	m_1	m_2	m_3	m_4	m_5	m_6	m_7	m_8	m_9	m_{10}
Distribution	LN									
Mean ($\times 10^5$ kg)	6.0	5.9	5.8	5.7	5.6	5.5	5.4	5.3	5.2	5.1
C.O.V.	0.10	0.10	0.10	0.10	0.10	0.10	0.10	0.10	0.10	0.10

LN = Lognormal; C.O.V. = coefficient of variation

292 of $\{A_i, B_i\}_{i=1}^{d_2}$ with the spectral representation, one can have a set of 625 representative samples of the fully non-
 293 stationary stochastic seismic accelerations. Three representative samples of the seismic acceleration time histories are
 294 shown in Fig. 7, where the non-stationary behavior in time domain can be clearly observed. Besides, the mean and
 295 standard deviation (Std.D) of 625 seismic acceleration samples against their targets are depicted in Fig. 8. As seen, the
 296 simulated results accord well with the targets, indicating the applicability of the LPSS based spectral representation.

297 Once the representative samples of the random structural properties and seismic excitation are produced, the
 298 deterministic dynamic structural analysis is performed repeatedly to extract samples of the EVD of concern. The
 299 ode45 function in Matlab is used to solve Eq. (35). Fig. 9 shows a typical sample of the restoring force v.s. inter-story
 300 drift, indicating a strong hysteretic behavior of the random structure under the fully non-stationary seismic excitations.

Table 2: Probabilistic information of the initial inter-story stiffness

Stiffness	k_1	k_2	k_3	k_4	k_5	k_6	k_7	k_8	k_9	k_{10}
Distribution	G	G	G	G	G	G	G	G	G	G
Mean ($\times 10^7$ N/m)	2.50	2.45	2.40	2.35	2.30	2.25	2.20	2.15	2.10	2.05
C.O.V.	0.15	0.15	0.15	0.15	0.15	0.15	0.15	0.15	0.15	0.15

\bar{G} = Gaussian

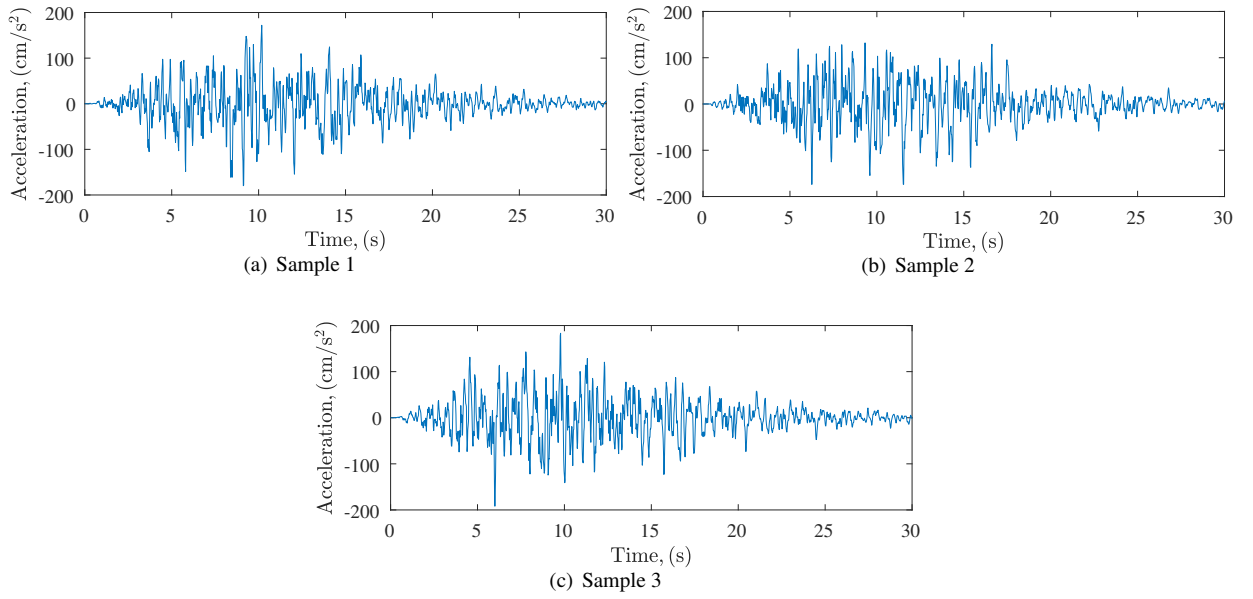


Figure 7: Representative samples of the fully non-stationary stochastic seismic acceleration.

301 In this study, we are especially interested in the EVDs of the 1-st, 5-th, and 10-th inter-story drift. The MGFs of
 302 interested EVDs computed by the LPSS method are depicted in Fig. 10, together with the reference results given
 303 by MCS (with 10^6 runs). It can be seen that all the three MGFs are accurately estimated since the 95% confidence
 304 intervals are very narrow and contain the corresponding reference results.

305 Based on the knowledge of the estimated MGFs, the EVDs can be recovered by the MTGIGD model. Figs. 11 - 13
 306 show the recovered PDF, CDF and probability of exceedance (POE) curves, where the results given by MCS (with 10^6
 307 runs) are also depicted for comparison. As seen, fairly good agreement can be observed between the results computed
 308 by the proposed method and those of MCS, indicating the accuracy of the proposed method for modeling not only the
 309 main body, but also the distribution tail of the EVD. From the POE curves, the first-passage failure probabilities under

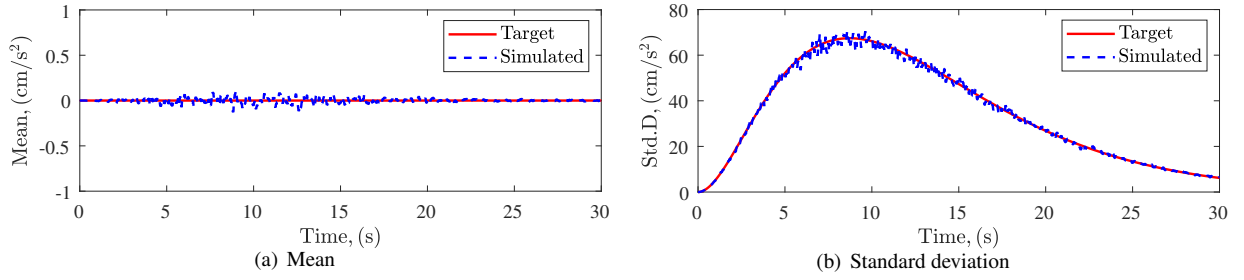


Figure 8: Comparison of the simulated mean and standard deviation with their targets for the fully non-stationary stochastic seismic excitation.

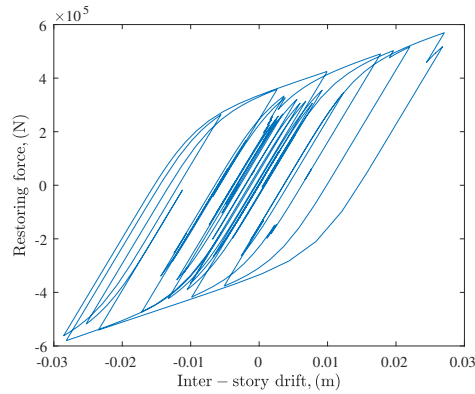


Figure 9: Typical hysteretic behavior for Example 3.

310 different thresholds can be simultaneously obtained. For example, the first-passage failure probabilities associated
 311 with the 1-st inter-story drift are listed in Tab. 3. In comparison with MCS, one can see that the proposed method
 312 can yield very accurate results, even for small failure probability levels less than 10^{-4} . Besides, the proposed method
 313 is much more efficient than MCS, since only $N = 625$ samples are required in this study. Finally, the EVD of the
 314 10-th inter-story drift is also approximated by the generalized extreme value distribution (GEVD) [17] with maximum
 315 likelihood estimation, shifted generalized lognormal distribution (SGLD) [44] with the method of moments (MOM)
 316 and maximum entropy method with four sample moments as constraint. Note that the same set of samples with the
 317 proposed method is employed in all these three methods. As shown in Fig. 14, large approximation errors appear,
 318 especially for the CDF and POE curves, raveling the limited flexibility of those parametric distribution models and/or
 319 inadequate parameter estimation methods.

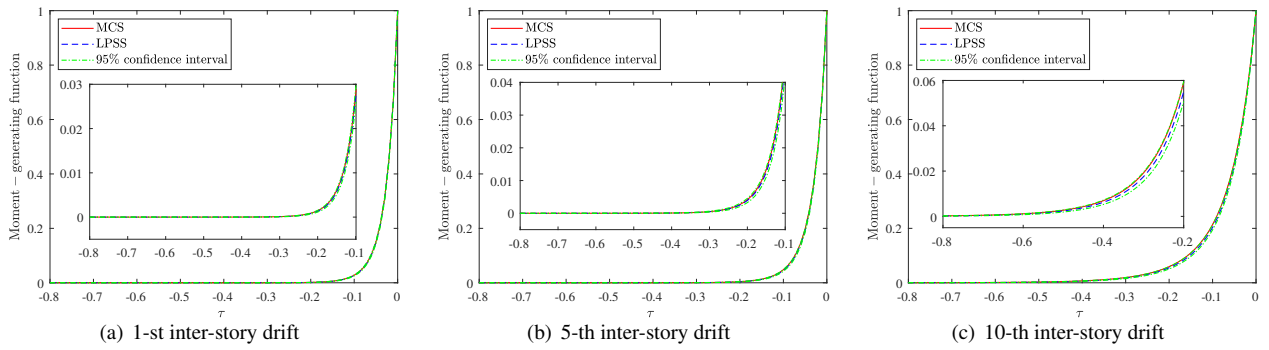


Figure 10: Moment-generating function of the EVD in Example 2.

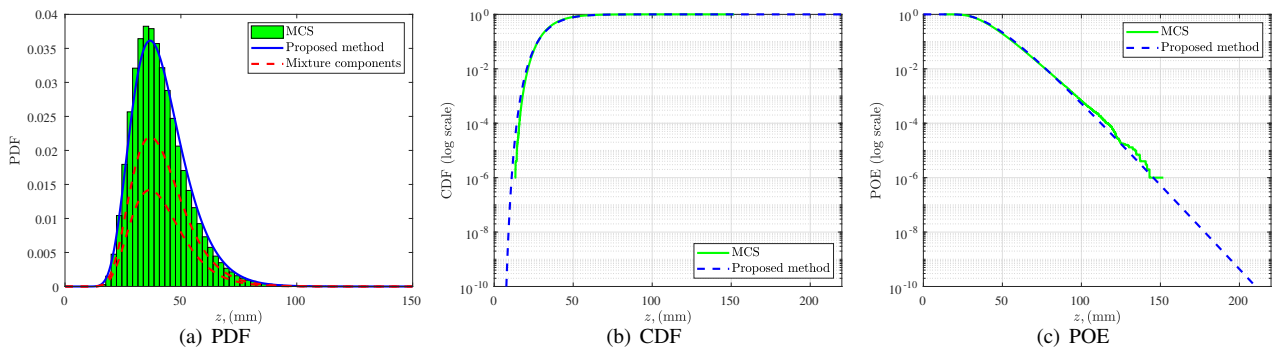


Figure 11: EVD of the 1-st inter-story drift.

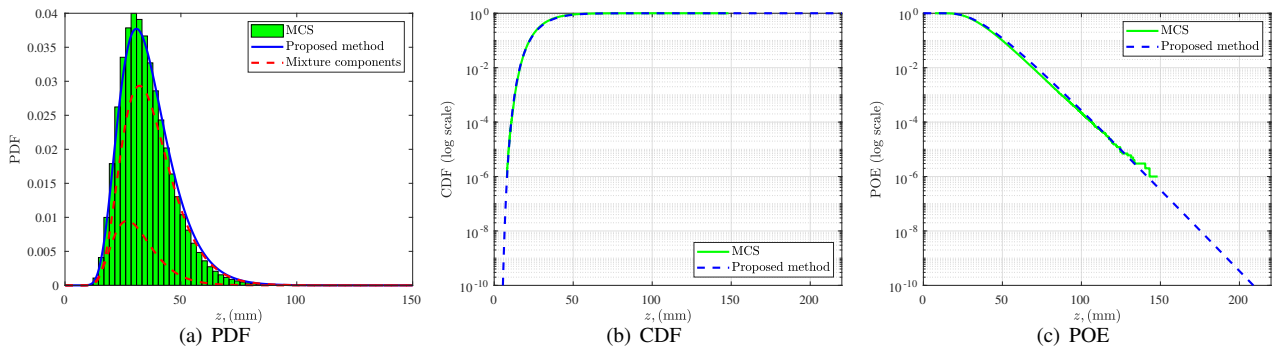


Figure 12: EVD of the 5-th inter-story drift.

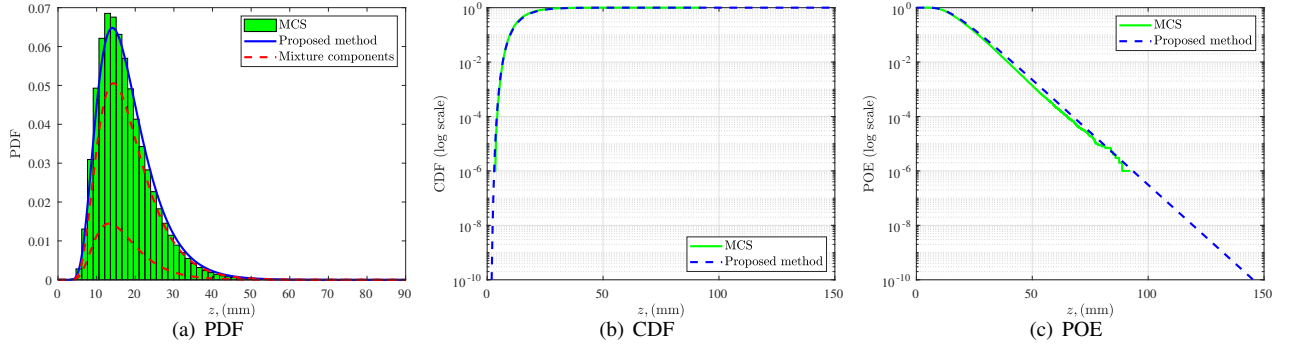


Figure 13: EVD of the 10-th inter-story drift.

Table 3: Comparison of the first-passage failure probabilities under different thresholds for example 2.

Method	N	Threshold (mm)						
		72	80	88	96	104	112	120
MCS	10^6	0.0181	0.0073	0.0028	1.1020×10^{-3}	4.2000×10^{-4}	1.8000×10^{-4}	5.9000×10^{-5}
Proposed	625	0.0194	0.0072	0.0026	9.0353×10^{-4}	3.0960×10^{-4}	1.0450×10^{-4}	3.4841×10^{-5}

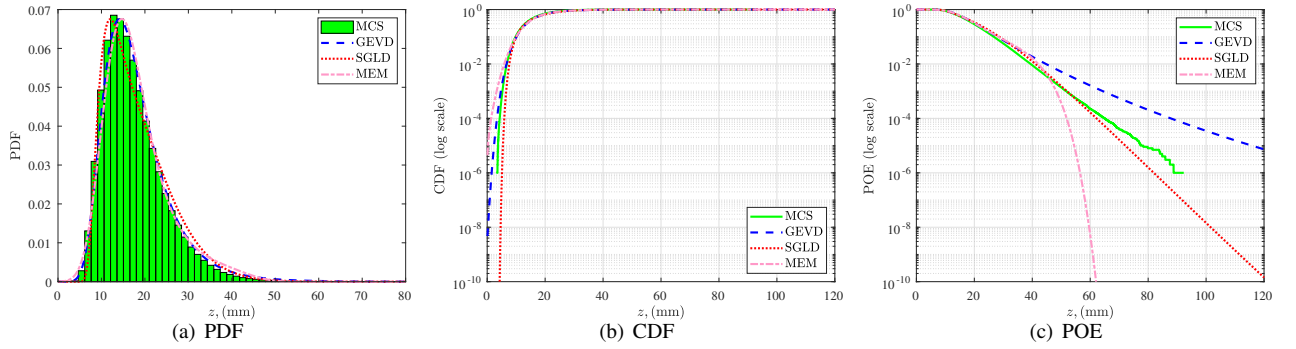


Figure 14: EVD of the 10-th inter-story drift by other methods.

320 5.3. Example 3: EVD and first-passage failure probabilities of a nonlinear bridge structure

321 A simplified two-span bridge structure is taken as the last example, as shown in Fig. 15. The bridge structure
 322 is modelled in OpenSees, an open software framework for earthquake engineering simulation. Since the beam is
 323 expected to remain linear elastic under seismic excitation, six elastic beam-column elements are used. The pier is

324 modelled by four nonlinear beam-column elements, the cross section of which is discretized into 225 fibers. Constitu-
 325 tive law of the material adopts the bilinear model, as depicted in the figure. The Rayleigh damping is employed with
 326 assuming the damping ratio of 3% for the first two modes. Eight random variables are consider in the structural prop-
 327 erties, whose information is listed in Tab. 4. For convenience, the same stochastic seismic excitations with example
 328 2 are applied to this model. Therefore, a total of $d = 1608$ random variables are actually contained in this example.
 329 The EVD of displacement at the pile top is of particular concern for seismic reliability analysis.

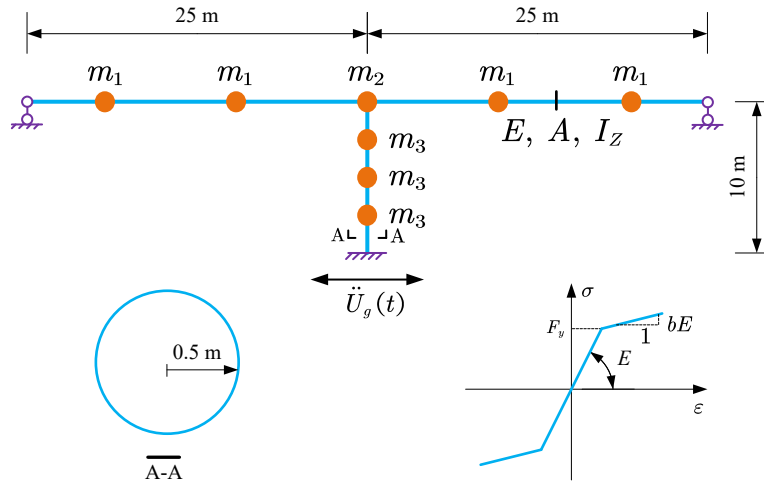


Figure 15: A two-span bridge structure subjected to stochastic seismic excitations.

330 Using the LPSS method with 625 samples, the MGF of the EVD is computed by repeatedly performing 625
 331 deterministic dynamic structural analyses. For comparison purposes, the crude MCS is also carried out to obtain the
 332 MGF (with 10^6 runs). As depicted in Fig. 16, it can be seen that the 95% confidence interval of the MGF is quite
 333 narrow and contains the result by MCS, indicating the accuracy of the estimated MGF.

334 The EVD can be recovered by the proposed mixture distribution, from the knowledge of the estimated MGF. In
 335 Fig. 17, one can observe that the PDF, CDF and POE in log scale are in good agreement with those reference results
 336 by crude MCS (with 10^6 runs). Note that we only perform 625 finite-element based structural dynamic analyses in
 337 this study. Therefore, the performance of the proposed method for recovering the EVD is demonstrated once again
 338 in terms of accuracy and efficiency. From the recove EVD, the first-passage failure probabilities under different
 339 prescribed thresholds can be obtained. As listed in Tab. 5, the results obtained from the proposed method accord

Table 4: Random variables for Example 3

Variable	Description	Distribution	Mean	C.O.V.
m_1	Lumped mass	LN	2.00×10^5 kg	0.10
m_2	Lumped mass	LN	2.05×10^5 kg	0.10
m_3	Lumped mass	LN	1.00×10^4 kg	0.10
A	Cross-sectional area of the beam	G	5.00×10^5 mm ²	0.05
I_Z	Moment of inertia of the beam	G	5.00×10^{12} mm ⁴	0.05
E	Young's modulus	G	2.05×10^5 Mpa	0.15
F_y	Yield stress	G	400 Mpa	0.15
b	Strain-hardening ratio	G	0.02	0.10

340 well with those by MCS, even for a low level of failure probability. Further, two recently developed methods are also
 341 implemented in this example, i.e., MIGLD with fractional moments [24] and mixture of two skew normal distributions
 342 (MTSND) with Laplace transform [37]. For fair comparison, the same EVD samples used for the proposed method
 343 are adopted to calculate the fractional moments and Laplace transform. Different from the original selection, note
 344 that the Laplace transform is evaluated at a new set of points, i.e., $\{s_i\}_{i=1}^7 = \{0.1, 0.2, 0.3, 0.4, 0.5, 0.6, 0.7\}$, so as
 345 to avoid very large numbers. The results by these two methods are compared with those by MCS in Fig. 18. Even
 346 though there are slight differences between the PDF curve and histogram, the MIGLD model can yield fairly good
 347 results concerning the CDF and PDF curves in log scale. On contrary, the MTSND model is unable to produce a
 348 comparative POE curve probably due to its limited capability for modelling an EVD. However, it would be difficult to
 349 identify which one is better among the MTGIGD and MIGLD for a general problem, and further research is required.

350 6. Conclusions and remarks

351 In this paper, an efficient approach is proposed for evaluation of the EVD and small first-passage failure prob-
 352 abilities of nonlinear structures with random parameters under stochastic seismic excitations. Unlike the traditional
 353 partial characterization, i.e., integer moments or fractional moments, the MGF is first introduced to characterize the

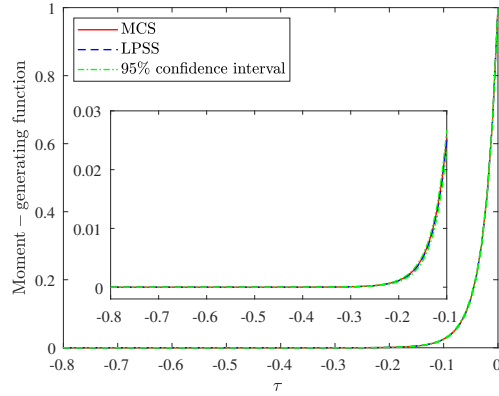


Figure 16: Moment-generating function of the EVD in Example 3.

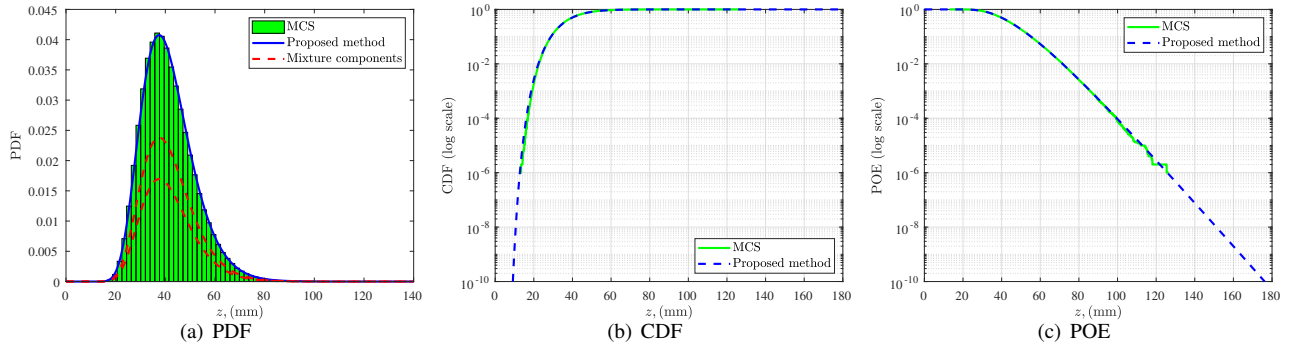


Figure 17: EVD of displacement at the pile top.

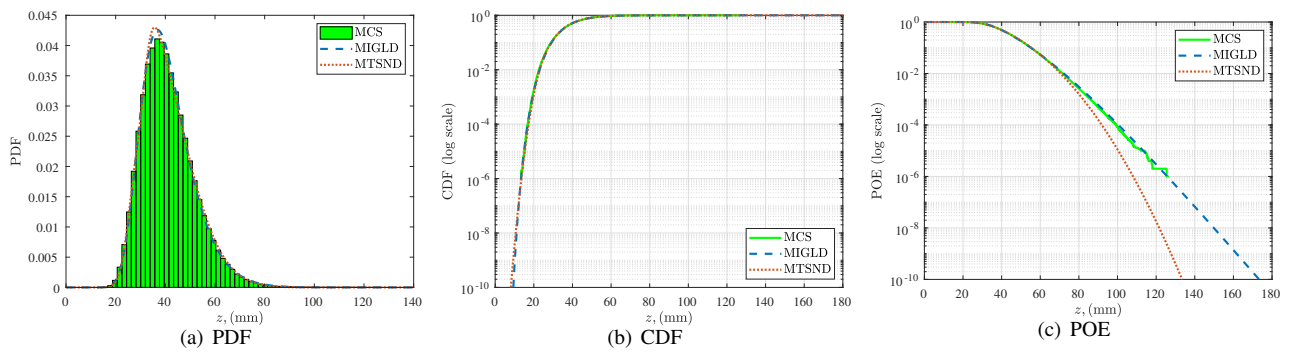


Figure 18: EVD of displacement at the pile top by other methods.

354 EVD of a general stochastic response process, which is usually defined as a high-dimensional expectation integral.

355 The advantages of MGF characterization are also demonstrated and discussed. Then, a recently developed variance-

Table 5: Comparison of the first-passage failure probabilities under different thresholds for Example 3.

Method	N	Threshold (mm)						
		60	68	76	84	92	100	108
MCS	10^6	0.0535	0.0171	0.0049	0.0014	3.5200×10^{-4}	8.1000×10^{-5}	1.9000×10^{-5}
Proposed	625	0.0531	0.0170	0.0050	0.0014	3.6637×10^{-4}	9.3851×10^{-5}	2.3420×10^{-5}

356 reduction sampling technique, named LPSS, is employed to estimate the MGF with a small sample size. Besides, the
357 unbiasedness of the estimator is proven and the confidence interval is given. To recover the EVD from the knowledge
358 of its estimated MGF, a versatile MTGIGD model is proposed. The close-form solution of MGF of the MTGIGD is
359 derived, and a novel parameter estimation technique based on the MGF is developed accordingly. Once the EVD is
360 reconstructed, the first-passage failure probabilities with different thresholds can be simultaneously obtained. Three
361 numerical examples are investigated to validate the proposed approach. The first example considers the EVD of
362 random variables, where the close-form solution of the EVD is available. A nonlinear shear frame structure and a
363 nonlinear bridge structure with random parameters subjected to fully non-stationary stochastic seismic excitations
364 are studied as another two examples. Results indicate that the proposed method: (1) is able to take both the ran-
365 domness from structural properties and external seismic excitations into consideration; (2) can be applied to very
366 high-dimensional stochastic dynamic systems; (3) is capable of capturing the EVD with high efficiency, not only the
367 main body, but also the distribution tail; (4) can yield very accurate estimation of the first-passage failure probabilities
368 under different prescribed thresholds, even for a small level less than 10^{-4} ; (5) is applicable for evaluation of multiple
369 EVDs in one single run.

370 Two main types of errors are included in the proposed approach. The first type is caused by the assumption on
371 parametric form for the EVD, which results in biased estimates and cannot be eliminated. Another type of error relates
372 to the fact that the MGF of EVD is evaluated by a sampling method. Since the estimator for the MGF is proven to be
373 unbiased, the latter error can be reduced by increasing the sample size.

374 **Declaration of competing interest**

375 The authors declare that they have no known competing financial interests or personal relationships that could
376 have appeared to influence the work reported in this paper.

377 **Acknowledgments**

378 The authors would like to appreciate the National Natural Science Foundation of China (NSFC 51905430) for
379 financially supporting the research. The first author also appreciates the support by the China Scholarship Council
380 (CSC).

381 **References**

- 382 [1] J. Song, A. Der Kiureghian, Joint first-passage probability and reliability of systems under stochastic excitation, *Journal of Engineering*
383 *Mechanics* 132 (1) (2006) 65–77.
- 384 [2] J. Li, J.-B. Chen, *Stochastic dynamics of structures*, John Wiley & Sons, 2009.
- 385 [3] R. Langley, A first passage approximation for normal stationary random processes, *Journal of Sound and Vibration* 122 (2) (1988) 261–275.
- 386 [4] J. He, Numerical calculation for first excursion probabilities of linear systems, *Probabilistic Engineering Mechanics* 24 (3) (2009) 418–425.
- 387 [5] J. Roberts, P. Spanos, Stochastic averaging: an approximate method of solving random vibration problems, *International Journal of Non-*
388 *Linear Mechanics* 21 (2) (1986) 111–134.
- 389 [6] Y. Zhao, An improved energy envelope stochastic averaging method and its application to a nonlinear oscillator, *Journal of Vibration and*
390 *Control* 23 (1) (2017) 119–130.
- 391 [7] A. Naess, V. Moe, Efficient path integration methods for nonlinear dynamic systems, *Probabilistic Engineering Mechanics* 15 (2) (2000)
392 221–231.
- 393 [8] A. Di Matteo, M. Di Paola, A. Pirrotta, Path integral solution for nonlinear systems under parametric poissonian white noise input, *Proba-*
394 *bilistic Engineering Mechanics* 44 (2016) 89–98.
- 395 [9] S.-K. Au, J. L. Beck, Estimation of small failure probabilities in high dimensions by subset simulation, *Probabilistic Engineering Mechanics*
396 16 (4) (2001) 263–277.
- 397 [10] H.-S. Li, Y.-Z. Ma, Z. Cao, A generalized subset simulation approach for estimating small failure probabilities of multiple stochastic re-
398 sponses, *Computers & Structures* 153 (2015) 239–251.
- 399 [11] J. Li, J.-B. Chen, W.-l. Fan, The equivalent extreme-value event and evaluation of the structural system reliability, *Structural Safety* 29 (2)
400 (2007) 112–131.

- 401 [12] B. Goller, H. Pradlwarter, G. Schuëller, Reliability assessment in structural dynamics, *Journal of Sound and Vibration* 332 (10) (2013)
402 2488–2499.
- 403 [13] M.-Z. Lyu, J.-B. Chen, A. Pirrotta, A novel method based on augmented markov vector process for the time-variant extreme value distribution
404 of stochastic dynamical systems enforced by poisson white noise, *Communications in Nonlinear Science and Numerical Simulation* 80 (2020)
405 104974.
- 406 [14] J.-B. Chen, M.-Z. Lyu, A new approach for time-variant probability density function of the maximal value of stochastic dynamical systems,
407 *Journal of Computational Physics* (2020) 109525.
- 408 [15] A. Naess, O. Gaidai, Estimation of extreme values from sampled time series, *Structural Safety* 31 (4) (2009) 325–334.
- 409 [16] A. Naess, O. Gaidai, Monte carlo methods for estimating the extreme response of dynamical systems, *Journal of Engineering Mechanics*
410 134 (8) (2008) 628–636.
- 411 [17] M. Grigoriu, G. Samorodnitsky, Reliability of dynamic systems in random environment by extreme value theory, *Probabilistic Engineering*
412 *Mechanics* 38 (2014) 54–69.
- 413 [18] Y.-G. Zhao, L.-W. Zhang, Z.-H. Lu, J. He, First passage probability assessment of stationary non-gaussian process using the third-order
414 polynomial transformation, *Advances in Structural Engineering* 22 (1) (2019) 187–201.
- 415 [19] T. Zhou, Y. Peng, Adaptive bayesian quadrature based statistical moments estimation for structural reliability analysis, *Reliability Engineering*
416 *& System Safety* (2020) 106902.
- 417 [20] J. Xu, S. Zhu, An efficient approach for high-dimensional structural reliability analysis, *Mechanical Systems and Signal Processing* 122
418 (2019) 152–170.
- 419 [21] J. Xu, C. Dang, A novel fractional moments-based maximum entropy method for high-dimensional reliability analysis, *Applied Mathematical*
420 *Modelling* 75 (2019) 749–768.
- 421 [22] Z.-Q. Chen, S.-X. Zheng, J. Zhang, C. Dang, K. Wei, X. Li, Efficient seismic reliability analysis of non-linear structures under non-stationary
422 ground motions, *Soil Dynamics and Earthquake Engineering* 139 (2020) 106385.
- 423 [23] U. Alibrandi, K. M. Mosalam, Kernel density maximum entropy method with generalized moments for evaluating probability distributions,
424 including tails, from a small sample of data, *International Journal for Numerical Methods in Engineering* 113 (13) (2018) 1904–1928.
- 425 [24] C. Dang, J. Xu, A mixture distribution with fractional moments for efficient seismic reliability analysis of nonlinear structures, *Engineering*
426 *Structures* 208 (2020) 109912.
- 427 [25] J. He, J. Gong, Estimate of small first passage probabilities of nonlinear random vibration systems by using tail approximation of extreme
428 distributions, *Structural Safety* 60 (2016) 28–36.
- 429 [26] J. Xu, Z. Ding, J. Wang, Extreme value distribution and small failure probabilities estimation of structures subjected to non-stationary
430 stochastic seismic excitations, *Structural Safety* 70 (2018) 93–103.
- 431 [27] J. Xu, J. Wang, D. Wang, Evaluation of the probability distribution of the extreme value of the response of nonlinear structures subjected to
432 fully nonstationary stochastic seismic excitations, *Journal of Engineering Mechanics* 146 (2) (2020) 06019006.
- 433 [28] J. Chen, J. Li, Extreme value distribution and reliability of nonlinear stochastic structures, *Earthquake Engineering and Engineering Vibration*

- 434 4 (2) (2005) 275–286.
- 435 [29] J.-B. Chen, J. Li, The extreme value distribution and dynamic reliability analysis of nonlinear structures with uncertain parameters, *Structural*
436 *Safety* 29 (2) (2007) 77–93.
- 437 [30] G. Chen, D. Yang, Direct probability integral method for stochastic response analysis of static and dynamic structural systems, *Computer*
438 *Methods in Applied Mechanics and Engineering* 357 (2019) 112612.
- 439 [31] M. D. Shields, J. Zhang, The generalization of latin hypercube sampling, *Reliability Engineering & System Safety* 148 (2016) 96–108.
- 440 [32] Z. Liu, Z. Liu, X. Ruan, Q. Zhang, Spectral representation-based dimension reduction for simulating multivariate non-stationary ground
441 motions, *Soil Dynamics and Earthquake Engineering* 114 (2018) 313–325.
- 442 [33] K. Phoon, H. Huang, S. Quek, Simulation of strongly non-gaussian processes using karhunen–loeve expansion, *Probabilistic Engineering*
443 *Mechanics* 20 (2) (2005) 188–198.
- 444 [34] J. Liang, S. R. Chaudhuri, M. Shinozuka, Simulation of nonstationary stochastic processes by spectral representation, *Journal of Engineering*
445 *Mechanics* 133 (6) (2007) 616–627.
- 446 [35] P. Billingsley, *Probability and Measure: Anniversary Edition*, Wiley, 2012.
- 447 [36] D. Zhou, X. Zhang, Y. Zhang, Dynamic reliability analysis for planetary gear system in shearer mechanisms, *Mechanism and Machine Theory*
448 105 (2016) 244–259.
- 449 [37] C. Dang, J. Xu, Unified reliability assessment for problems with low- to high-dimensional random inputs using the laplace transform and a
450 mixture distribution, *Reliability Engineering & System Safety* (2020) 107124.
- 451 [38] B. Jorgensen, *Statistical properties of the generalized inverse Gaussian distribution*, Vol. 9, Springer Science & Business Media, 2012.
- 452 [39] J. L. Folks, R. S. Chhikara, The inverse gaussian distribution and its statistical application—a review, *Journal of the Royal Statistical Society:*
453 *Series B (Methodological)* 40 (3) (1978) 263–275.
- 454 [40] G. J. McLachlan, D. Peel, *Finite mixture models*, John Wiley & Sons, 2004.
- 455 [41] Y.-K. Wen, Method for random vibration of hysteretic systems, *Journal of the Engineering Mechanics Division* 102 (2) (1976) 249–263.
- 456 [42] Y. K. Wen, Equivalent Linearization for Hysteretic Systems Under Random Excitation, *Journal of Applied Mechanics* 47 (1980) 150–154.
- 457 [43] Z. Liu, W. Liu, Y. Peng, Random function based spectral representation of stationary and non-stationary stochastic processes, *Probabilistic*
458 *Engineering Mechanics* 45 (2016) 115–126.
- 459 [44] Y. M. Low, A new distribution for fitting four moments and its applications to reliability analysis, *Structural Safety* 42 (2013) 12–25.